Positon and hybrid solutions for the (2+1)-dimensional complex modified Korteweg–de Vries equations

Feng Yuan(袁丰)[1,†] and Behzad Ghanbari[2]

[1] *College of Science, Nanjing University of Posts and Telecommunications, Nanjing* 210023, *China*
[2] *Department of Basic Science, Kermanshah University of Technology, Kermanshah, Iran*

(Received 2 August 2022; revised manuscript received 6 September 2022; accepted manuscript online 21 September 2022)

Solving nonlinear partial differential equations have attracted intensive attention in the past few decades. In this paper, the Darboux transformation method is used to derive several positon and hybrid solutions for the (2+1)-dimensional complex modified Korteweg–de Vries equations. Based on the zero seed solution, the positon solution and the hybrid solutions of positon and soliton are constructed. The composition of positons is studied, showing that multi-positons of (2+1)-dimensional equations are decomposed into multi-solitons as well as the (1+1)-dimensions. Moreover, the interactions between positon and soliton are analyzed. In addition, the hybrid solutions of b-positon and breather are obtained using the plane wave seed solution, and their evolutions with time are discussed.

Keywords: positon solution, b-positon solution, breather solution, the hybrid solution, the Darboux transformation

PACS: 02.30.Ik, 02.30.Jr, 05.45.–a **DOI:** 10.1088/1674-1056/ac935b

1. Introduction

Nonlinear evolution equations (NLEEs) and their exact solutions play a substantial role in describing many nonlinear phenomena arising in physical applications.[1–5] The so-called positon is a fundamental solution of NLEEs on zero background, which was first proposed in the KdV equation.[6] Further, it was extended to other equations such as the Sine–Gordon equation,[7,8] the modified KdV equation,[9,10] the NLS-MB equations.[11] Positon can be viewed as a long-range analog of multi-soliton and slowly decay,[12] which are derived from the multi-soliton by the limits $\lambda_{2j-1} \to \lambda_1$ and $\lambda_{2j} \to \lambda_2$ (λ_j is the eigenvalue of Lax pair).[11] If part of λ_{2j-1} tents to λ_1, the hybrid solution of positon and soliton can be obtained.[13–15] Similarly, if make part of breathers degenerate, the hybrid solutions of b-positon and breather on the nonzero background can be obtained based on plane wave seed solutions. These solutions have been studied extensively in (1+1)-dimensions but rarely studied in (2+1)-dimensions. In this paper, the positon solution, the hybrid solution of positon and soliton, and the hybrid solution of b-positon and breather for a (2+1)-dimensional NLEE are extracted with the aid of the degenerate Darboux transformation (DT) method. After applying the method, rational solutions, positon solutions, b-positon solutions, and hybrid solutions of them are determined.[16–19]

Whenever there are dispersion and nonlinear terms in NLEEs, the existence of multi-solutions of the interaction form such as the interaction between solitons and breathers, rogue waves and breathers, rogue waves and lumps will be probable.[20–24] These interactions occur in some practical applications such as phase transition, amplitude superposition, elastic and inelastic collision, and change of propagation direction. Therefore, the interaction analysis of multi-solutions is of great significance to understand the properties of NLEEs.

Recently, a (2+1)-dimensional complex modified Korteweg–de Vries (cmKdV) equation has been proposed by Yesmakhanova,[25] which appears in the description of some problems in applied magnetism and nanophysics. These (2+1)-D cmKdV equations can be formulated as

$$\begin{cases} q_t + q_{xxy} + (qw)_x + \mathrm{i}qv = 0, \\ v_x + 2\mathrm{i}(q_{xy}q^* - qq^*_{xy}) = 0, \\ w_x - 2(|q|^2)_y = 0. \end{cases} \tag{1}$$

Also, their corresponding Lax pair is derived as

$$\Psi_x = A\Psi, \quad \Psi_t = 4\lambda^2\Psi_y + B\Psi, \tag{2}$$

where

$$A = \lambda J + A_0, \quad B = \lambda B_1 + B_0,$$
$$\Psi = \begin{bmatrix} \psi_1(\lambda,x,y,t) \\ \psi_2(\lambda,x,y,t) \end{bmatrix}, \quad J = \begin{bmatrix} -\mathrm{i} & 0 \\ 0 & \mathrm{i} \end{bmatrix},$$
$$A_0 = \begin{bmatrix} 0 & q \\ -r & 0 \end{bmatrix},$$
$$B_0 = \begin{bmatrix} -\mathrm{i}v/2 & -q_{xy} - wq \\ r_{xy} + wr & \mathrm{i}v/2 \end{bmatrix},$$
$$B_1 = \begin{bmatrix} \mathrm{i}w & 2\mathrm{i}q_y \\ 2\mathrm{i}r_y & -\mathrm{i}w \end{bmatrix}.$$

Here $r = q^*$, $\lambda \in \mathbb{C}$, λ is the eigenvalue of Eq. (2), and * denotes the complex conjugation operator. Equation (1) can be modified to $q_t + q_{xxy} + 2q_x \int (|q|^2)_y \mathrm{d}x + 2q(|q|^2)_y -$

†Corresponding author. E-mail: yf2017@mail.ustc.edu.cn; fengyuan@njupt.edu.cn

© 2023 Chinese Physical Society and IOP Publishing Ltd

$2iq\int(q_{xy}q^*-qq^*_{xy})\,dx=0$, so we confine our study in this article exclusively on q.

The (2+1)-D cmKdV equations have been studied in several articles by the DT method. Starting with the zero seed, the soliton and deform soliton solutions have been obtained in Refs. [26,27]. On the other hand, the periodic solutions are studied in Refs. [28,29] based on a plane wave seed. In Ref. [30] Zhu studied the nonlocal reductions. In Ref. [29] Yuan studied the degenerate breather solution by the first degeneration (i.e., the limit $\lambda_{2k-1}\to\lambda_1$) and discussed the degeneration progress in detail. The rational solutions of these (2+1)-D cmKdV equations, including the rogue wave solutions and the lump solutions, have been studied in Ref. [31]. In this paper, we aim to study the multi-positon solutions and some hybrid solutions, and analyze their properties such as composition, the influence of parameters, and dynamical properties through the degenerate DT transformation.

2. Composition of positon solutions

The order-n solution of Eq. (1) generated by Darboux transformation from a seed solution $q^{[0]}$, $w^{[0]}$, $v^{[0]}$ is given as follows:[27–29]

$$q^{[n]}=q^{[0]}-2i\frac{D_{2n}}{W_{2n}},\tag{3}$$

where

$$W_{2n}=\begin{vmatrix}\psi_{11}&\psi_{12}&\cdots&\lambda_1^{n-1}\psi_{11}&\lambda_1^{n-1}\psi_{12}\\ \psi_{21}&\psi_{22}&\cdots&\lambda_2^{n-1}\psi_{21}&\lambda_2^{n-1}\psi_{22}\\ \vdots&\vdots&\ddots&\vdots&\vdots\\ \psi_{2n,1}&\psi_{2n,2}&\cdots&\lambda_{2n}^{n-1}\psi_{2n,1}&\lambda_{2n}^{n-1}\psi_{2n,2}\end{vmatrix},$$

$$D_{2n}=\begin{vmatrix}\psi_{11}&\psi_{12}&\cdots&\lambda_1^{n-1}\psi_{11}&\lambda_1^{n}\psi_{11}\\ \psi_{21}&\psi_{22}&\cdots&\lambda_2^{n-1}\psi_{21}&\lambda_2^{n}\psi_{21}\\ \vdots&\vdots&\ddots&\vdots&\vdots\\ \psi_{2n,1}&\psi_{2n,2}&\cdots&\lambda_{2n}^{n-1}\psi_{2n,1}&\lambda_{2n}^{n}\psi_{2n,1}\end{vmatrix},\tag{4}$$

and $[\psi_{j1},\ \psi_{j2}]^{\mathrm{T}}$ is a set of eigenfunctions corresponding to $\lambda=\lambda_j$.

Starting from the seed solution $q^{[0]}=0$, the eigenfunctions associated with λ_j can be derived as the following form:

$$\begin{aligned}\psi_{2l-1,1}&=e^{-i\lambda_{2l-1}x+\mu_{2l-1}(y+4\lambda_{2l-1}^2t)+\zeta_l},\\ \psi_{2l,1}&=e^{-i\lambda_{2l}x-\mu_{2l}(y+4\lambda_{2l}^2t)-\zeta_l},\\ \psi_{2l-1,2}&=e^{i\lambda_{2l-1}x-\mu_{2l-1}(y+4\lambda_{2l-1}^2t)-\zeta_l},\\ \psi_{2l,2}&=-e^{i\lambda_{2l}x+\mu_{2l}(y+4\lambda_{2l}^2t)+\zeta_l}.\end{aligned}\tag{5}$$

Here $\lambda_{2l-1}=\lambda_{2l}^*$, $\mu_{2l-1}=\mu_{2l}^*$, ζ_l $(l=1,\ldots,n)$ is real. Substituting Eq. (5) and $q^{[0]}=0$ into Eq. (3), the n-soliton solution can be obtained. For (1+1)-dimensional NLEEs, the n-positon solutions have been obtained through the limits $\lambda_{2l-1}\to\lambda_1$.[32,33] By the same method, the n-positon solutions for the (2+1)-D cmKdV equations can be constructed.

Theorem 1 The n-positon solution for the (2+1)-D cmKdV equations is

$$q_p^{[n]}=-2i\frac{\Delta_{11}}{\Delta_{12}},\tag{6}$$

where

$$\begin{aligned}\Delta_{11}&=\left(\frac{\partial^{n_j}}{\partial\varepsilon^{n_j}}\Big|_{\varepsilon=0}(D_{2n})_{jk}(\lambda_j+\varepsilon)\right)_{2n\times 2n},\\ \Delta_{12}&=\left(\frac{\partial^{n_j}}{\partial\varepsilon^{n_j}}\Big|_{\varepsilon=0}(W_{2n})_{jk}(\lambda_j+\varepsilon)\right)_{2n\times 2n},\\ \lambda_{2l-1}&=\lambda_1,\quad l=1,\ldots,n,\\ n_j&=\left[\frac{j-1}{2}\right],\quad j=1,\ldots,2n.\end{aligned}$$

Here $[\ \ ]$ means taking the integer part, D_{2n} and W_{2n} are given in Eq. (4) and ψ_{jk} are given in Eq. (5).

2.1. Composition of 2-positon solutions

Substituting $n=2$, $\lambda_1=\alpha_1+\beta_1 i$, $\lambda_2=\alpha_1-\beta_1 i$, $\mu_1=a_1+b_1 i$, $\mu_2=a_1-b_1 i$ into Eq. (6), the 2-positon solution can be simplified to

$$|q_p^{[2]}|^2=\frac{64\beta_1^2((\xi_4+4\beta_1\xi_1+1)e^{-4\xi_3}+(\xi_4-4\beta_1\xi_1+1)e^{4\xi_3}-8\beta_1^2(\xi_1^2-64\xi_2^2t^2)+2)}{(e^{4\xi_3}+e^{-4\xi_3}+4\xi_4+2)^2},\tag{7}$$

where $\xi_1=x-8a_1\beta_1t-8\alpha_1b_1t$, $\xi_2=a_1\alpha_1-b_1\beta_1$, $\xi_3=\beta\xi_1+a_1(y+4t(\alpha_1^2+\beta_1^2))+\zeta_1$, $\xi_4=4\beta_1^2(\xi_1^2+64\xi_2^2t^2)$. It is easy to verify $|q^{[2]}(x,y,t)|=|q^{[2]}(-x,-y-(2\zeta_1/a_1),-t)|$, so we just consider the evolution with $t\geqslant 0$.

Figure 1 depicts the density figures of Eq. (7) with different moments. On the moment $t=0$, the interaction of the two units of the positon solution is most strongly (see Fig. 1(a)), and the positon reaches the maximum amplitude $4\beta_1$ at the point $(0,\ -2\zeta_1/a_1)$ on (x,y)-plane. As t increases, both two units of the positon gradually separate and their interactions weaken (see Figs. 1(b) and 1(c)). After that, the two units are completely separated at $t\to\infty$ and the positon is represented as two identical bound solitons (see Fig. 1(d)). Further, ζ_1 does not affect the velocity and shape of the positon, and it just affects the location of the maximum amplitude (see Fig. 2).

As we know, for the (1+1)-dimensional NLLEs, the n-positon solution can be viewed as the superposition of n-solitons as $|t|\gg 0$. Next, we discuss the decomposition of

the 2-positon Eq. (7) with $\zeta_1 = 0$ in a similar way. The order-1 soliton solution of Eq. (1) can be expressed as

$$|q_s^{[1]}| = \frac{4\beta\, \mathrm{e}^{2\xi_3}}{1+\mathrm{e}^{4\xi_3}}. \tag{8}$$

The 2-positon Eq. (7) can be decomposed asymptotically as

$$|q_p^{[2]}|^2 \approx |q_s^{[1]}(\xi_3 + c_1)|^2 + |q_s^{[1]}(\xi_3 - c_1)|^2, \quad |y| \to \infty, \tag{9}$$

where c_1 is the "phase shift" which can be fixed later. Substituting $t = 0$ into Eq. (9) and considering the approximation of this equation in the neighborhood of $\xi_3 = 0$, we can find that $c_1 \approx -\frac{1}{4}\ln(16a_1^2y^2+1)$. The precise approximate trajectories are two curves defined by $\xi_3 \pm c_1 = 0$, which are shown in Fig. 3. For any given parameter and t, one can decompose it in the same way. Figure 4 demonstrates the approximate trajectories with different moments, and the phase shifts are given as

$$\begin{aligned}
\text{(a)}\ c_1 &\approx \frac{1}{4}\ln\left(72y^2+5676y+\frac{230711}{2}\right.\\
&\quad \left.+6y\sqrt{144y^2+22704y+1356338}\right),\\
\text{(b)}\ c_1 &\approx \frac{1}{4}\ln\left(72y^2+11352y+460075\right.\\
&\quad \left.+12y\sqrt{36y^2+11352y+1354991}\right),\\
\text{(c)}\ c_1 &\approx \frac{1}{4}\ln\left(72y^2+28380y+\frac{5746223}{2}\right.\\
&\quad \left.+6y\sqrt{144y^2+113520y+33865346}\right).
\end{aligned} \tag{10}$$

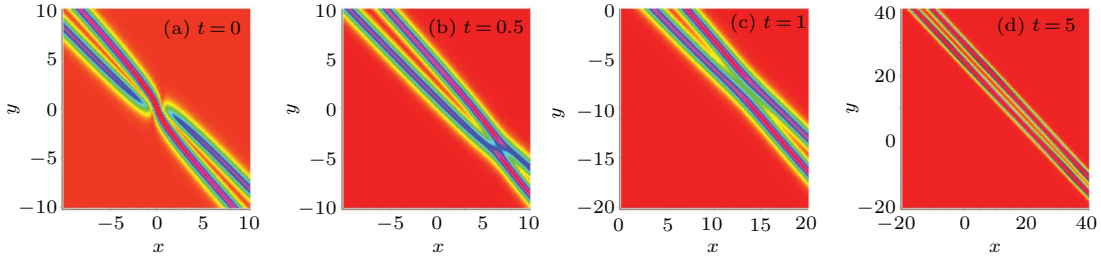


Fig. 1. The density figures of $|q_p^{[2]}|$ with $a_1 = 1$, $b_1 = 2/3$, $\zeta_1 = 0$, $\alpha_1 = 1$, $\beta_1 = 1$: (a) $t = 0$, (b) $t = 0.5$, (c) $t = 1$, (d) $t = 5$.

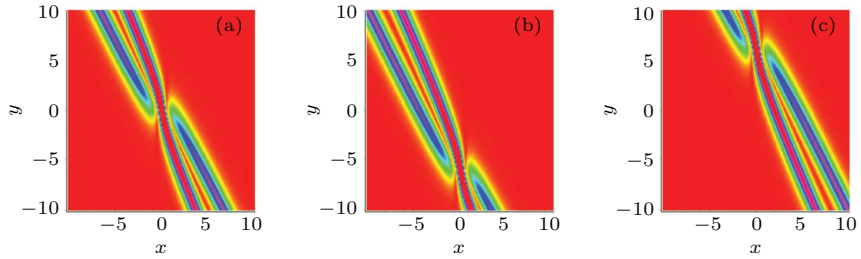


Fig. 2. The density figures of $|q_p^{[2]}|$ with $a_1 = 1/2$, $b_1 = 2/3$, $\alpha_1 = 3$, $\beta_1 = 1$, $t = 0$: (a) $\zeta_1 = 0$, (b) $\zeta_1 = 3$, (c) $\zeta_1 = -3$.

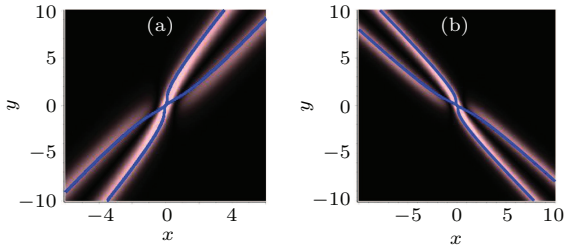


Fig. 3. The density figures of $|q_p^{[2]}|$ with $t = 0$: (a) $a_1 = -1/2$, $b_1 = 2/3$, $\alpha_1 = 1$, $\beta_1 = 1$, $\zeta_1 = 0$, (b) $a_1 = 4/5$, $b_1 = 1/5$, $\alpha_1 = 1/2$, $\beta_1 = 4/5$, $\zeta_1 = 0$. The blue curves are the trajectories $\xi_3 \pm c_1 = 0$.

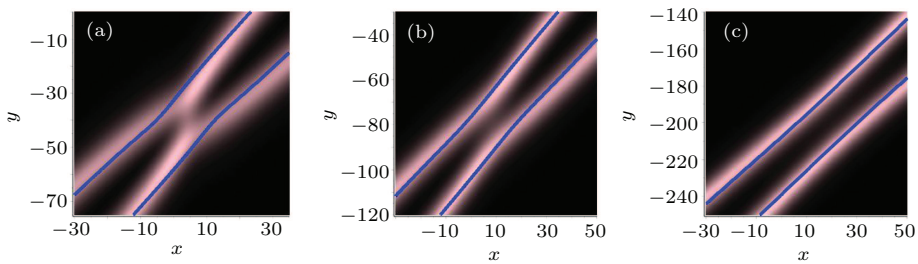


Fig. 4. The density figures of $|q_p^{[2]}|$ with $a_1 = 2/3$, $b_1 = 1/4$, $\alpha_1 = -1/5$, $\beta_1 = 1/3$, $\zeta_1 = 0$: (a) $t = 3$, (b) $t = 6$, (c) $t = 15$. The blue curves are the trajectories $\xi_3 \pm c_1 = 0$ with Eq. (10).

2.2. Composition of 3-positon solutions

Substituting $n=3$, $\lambda_1=\alpha_1+\beta_1\mathrm{i}$, $\lambda_2=\alpha_1-\beta_1\mathrm{i}$, $\mu_1=a_1+b_1\mathrm{i}$, $\mu_2=a_1-b_1\mathrm{i}$ into Eq. (6), the 3-positon solution can be obtained. The 3-positon can be decomposed asymptotically as

$$|q_p^{[3]}|^2 \approx |q_s^{[1]}(\xi_3+c_2)|^2+|q_s^{[1]}|^2+|q_s^{[1]}(\xi_3-c_2)|^2, \quad |y|\to\infty, \tag{11}$$

where c_2 is the "phase shift" which can be fixed later. Because of the complexity of the formula and the huge amount of calculation, only the decomposition of order-3 positon solutions at $t=0$ will be discussed here. Substituting $t=0$ into Eq. (11), and considering the approximation of this equation in the neighborhood of $\xi_3=0$, it reads $c_2\approx-(1/4)\ln(64a_1^4y^4+1)$. The precise approximate trajectories are three curves defined by $\xi_3\pm c_2=0$ and $\xi_3=0$, as shown in Fig. 5.

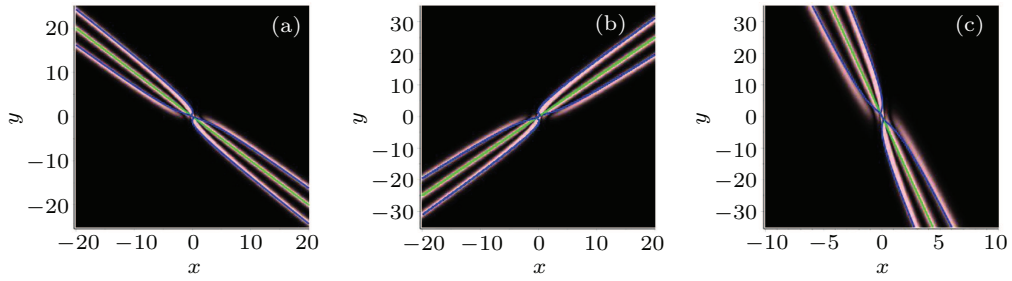


Fig. 5. The density figures of $|q_p^{[3]}|$ with $t=0$: (a) $a_1=1$, $b_1=1$, $\alpha_1=1$, $\beta_1=1$, $\zeta_1=0$, (b) $a_1=-2/3$, $b_1=1/4$, $\alpha_1=1$, $\beta_1=5/6$, $\zeta_1=0$, (c) $a_1=1/4$, $b_1=1$, $\alpha_1=1$, $\beta_1=2$, $\zeta_1=0$. The blue curves are the approximate trajectories $\xi_3\pm c_2=0$ and the green curve is the approximate trajectory $\xi_3=0$.

Through the above analysis, we obtain that the n-positon solution of the (2+1)-dimensional equations can also be decomposed into n identical solitons which are parallel to each other. Different from the (1+1)-dimension, the 2-dimensional positon has the strongest interaction at $t=0$, showing two crossing solitons. As $t\to\infty$, the interaction disappears and it behaves as n parallel solitons.

3. Hybrid solutions on zero background

In this section, two kinds of interaction are introduced: the interaction between positon and soliton, and the interaction between positons.

3.1. Interaction between positon and soliton solutions

The hybrid solution consisting of positon and soliton will be derived through the limits $\lambda_{2j-1}\to\lambda_1=-\alpha_1+\beta_1\mathrm{i}$ $(j=1,\ldots,m,\ m\leqslant n-1)$ in Eq. (3), and the interaction between positon and soliton will be obtained.

Theorem 2 The order-n hybrid solution consisting of m-positon and l-soliton for the (2+1)-D cmKdV equations is

$$q_{mp-ls}^{[n]}=-2\mathrm{i}\frac{\Delta_{21}}{\Delta_{22}}, \tag{12}$$

with

$$\Delta_{21}=\left(\frac{\partial^{n_j}}{\partial\varepsilon^{n_j}}\Big|_{\varepsilon=0}(D_{2n})_{jk}(\lambda_j+\varepsilon)\right)_{2n\times 2n},$$
$$\Delta_{22}=\left(\frac{\partial^{n_j}}{\partial\varepsilon^{n_j}}\Big|_{\varepsilon=0}(W_{2n})_{jk}(\lambda_j+\varepsilon)\right)_{2n\times 2n},$$
$$\lambda_{2l-1}=\lambda_1\,(l\leqslant m),\quad n=m+l,$$
$$n_j=\begin{cases}\left[\dfrac{j-1}{2}\right], & j\leqslant 2m,\\ 0, & j>2m,\end{cases}$$

where $[\ \ ]$ means taking the integer part. D_{2n} and W_{2n} are given in Eq. (4), and ψ_{jk} are given in Eq. (5).

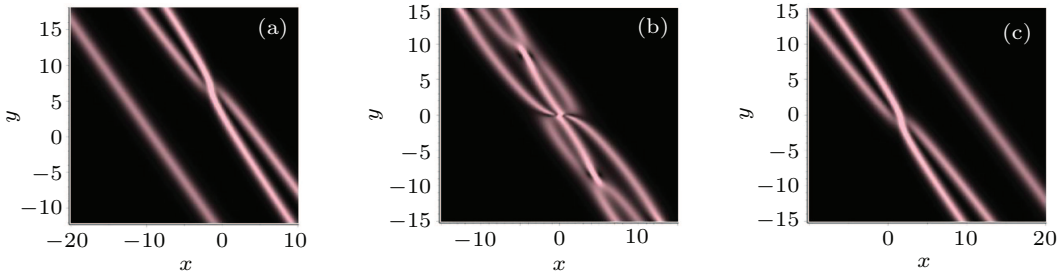


Fig. 6. The density figures of order-3 hybrid solution with $t=0$, $\lambda_1=\lambda_3=2/5+\mathrm{i}$, $\lambda_5=1/3+3\mathrm{i}/4$, $\mu_1=\mu_3=2/3+\mathrm{i}/4$, $\mu_5=1/2+\mathrm{i}/2$: (a) $\zeta_1=-2$, $\zeta_2=5$, (b) $\zeta_1=0$, $\zeta_2=0$, (c) $\zeta_1=-2$, $\zeta_2=-7$.

Choosing $n=3$, $m=2$ in Eq. (12), the order-3 hybrid solution consisting of 2-positon and 1-soliton is obtained. Figure 6 shows the density figures of order-3 hybrid solutions with the same parameters except ζ_j. Figure 7 shows the interaction between positon and soliton at different times. On the moment $t=0$, the positon and soliton interact most strongly, and the maximum amplitude $4\beta_1+2\beta_3$ is reached in the central region (see Fig. 7(a)). As time increases, the positon and soli-

ton move at a different speed. The interaction between the two units of the positon and the interaction between the positon and the soliton gradually diminishes (see Figs. 7(b) and 7(c)). When $t \gg 0$, the interaction between positon and soliton is almost negligible, and the hybrid solution is represented by a 2-soliton and a 1-soliton (see Fig. 7(d)).

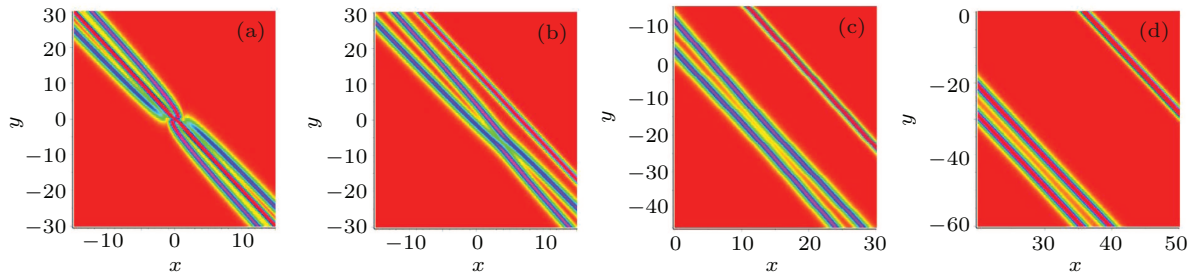


Fig. 7. The density figures of order-3 hybrid solution with $\zeta_1=0$, $\zeta_2=0$, $\lambda_1=\lambda_3=4/5+\mathrm{i}$, $\lambda_5=1/2+5\mathrm{i}/3$, $\mu_1=\mu_3=1/2+\mathrm{i}/10$, $\mu_5=5/6+\mathrm{i}/5$: (a) $t=0$, (b) $t=1$, (c) $t=3$, (d) $t=6$.

3.2. Interaction between positon solutions

A hybrid positon solution will be provided by the following theorem to discuss the interaction between positons associated with different eigenvalues.

Theorem 3 The order-n hybrid solution for the (2+1)-D cmKdV equations consisting of m-positon and l-politon is

$$q^{[n]}_{mp-lp}=-2\mathrm{i}\frac{\Delta_{31}}{\Delta_{32}}, \tag{13}$$

with

$$\Delta_{31}=\left(\frac{\partial^{n_j}}{\partial\varepsilon^{n_j}}\Big|_{\varepsilon=0}(D_{2n})_{jk}(\lambda_j+\varepsilon)\right)_{2n\times 2n},$$
$$\Delta_{32}=\left(\frac{\partial^{n_j}}{\partial\varepsilon^{n_j}}\Big|_{\varepsilon=0}(W_{2n})_{jk}(\lambda_j+\varepsilon)\right)_{2n\times 2n},$$
$$n=m+l,\quad \lambda_{2l-1}=\begin{cases}\lambda_1, & l\leqslant m,\\ \lambda_{2m+1}, & l>m,\end{cases}$$
$$n_j=\begin{cases}\left[\dfrac{j-1}{2}\right], & j\leqslant 2m,\\ \left[\dfrac{j-1}{2}\right]-m, & j>2m,\end{cases}$$

where $[\ \ ]$ means taking the integer part and $\lambda_1\neq\lambda_{2m+1}$. D_{2n} and W_{2n} are given in Eq. (4), and ψ_{jk} are given in Eq. (5).

Choosing $n=4$, $m=2$, $\lambda_1\neq\lambda_{2m+1}$ in Eq. (13), the order-4 hybrid positon solution consisting of two 2-positons can be obtained, as shown in Fig. 8.

□ When $\zeta_1=\zeta_2=0$ and $\beta_1/a_1=\beta_3/a_3$, the result described in Fig. 8(a) can be generated. This kind of hybrid positon has the strongest interaction at $t=0$ in the whole (x,y)-plane and the centers of the two positons coincide with each other, which are circled in black in Fig. 8(a).

□ When $\zeta_1\neq\zeta_2$ and $\beta_1/a_1=\beta_3/a_3$, the result described in Fig. 8(b) can be generated. This kind of hybrid positon looks like two separate positon at $t=0$, and the interaction is weak in the whole (x,y)-plane. The centers of the two positons have no superposition, which are circled in black in Fig. 8(b).

□ When $\zeta_1=\zeta_2=0$ and $\beta_1/a_1\neq\beta_3/a_3$, the result described in Fig. 8(c) can be generated. This kind of hybrid positon looks like two intersecting positon at $t=0$, and the centers of the two positons are overlapped, which are circled in black in Fig. 8(c).

□ When $\zeta_1\neq\zeta_2$ and $\beta_1/a_1\neq\beta_3/a_3$, the result described in Fig. 8(d) can be generated. This kind of hybrid positon looks like two intersecting positon at $t=0$, and the centers of the two positons do not overlap, which are circled in black in Fig. 8(d).

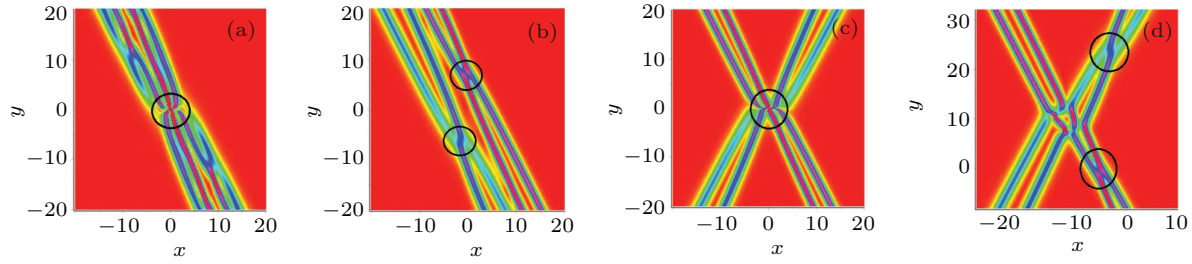


Fig. 8. The density figures of $q^{[4]}_{2p-2p}$, and the centers of positons marked with black circles, for parameters $t=0$, $\lambda_1=1/5+\mathrm{i}$, $\lambda_5=2/3+2\mathrm{i}/3$, $\mu_1=\mu_3=1/2+\mathrm{i}/5$: (a) $\zeta_1=0$, $\zeta_2=0$, $\mu_5=\mu_7=1/3+\mathrm{i}/4$; (b) $\zeta_1=-2$, $\zeta_2=2$, $\mu_5=\mu_7=1/3+\mathrm{i}/4$; (c) $\zeta_1=0$, $\zeta_2=0$, $\mu_5=\mu_7=-1/3+\mathrm{i}/4$; (d) $\zeta_1=2$, $\zeta_2=8$, $\mu_5=\mu_7=-1/3+\mathrm{i}/4$.

4. Hybrid solutions on nonzero background

Starting with the plane wave seed solution $q^{[0]}=c\mathrm{e}^{\mathrm{i}\rho}$, $w^{[0]}=0$, $v^{[0]}=0$ ($\rho=ax+by+a^2bt$, a, b, c are real constants), n sets of eigenfunctions for Eq. (2) corresponding with eigenvalues $\lambda_{2j-1}=-a/2+\beta_j\mathrm{i}=\lambda^*_{2j}$ ($\beta_j\in\mathbb{R}$, $j=1,\ldots,n$) have been given in Refs. [28,29] as follows:

$$\psi_{2j-1,1}=\mathrm{e}^{\frac{\mathrm{i}\rho}{2}}\left(c\mathrm{e}^{\mathrm{i}\theta_{2j-1}}+\mathrm{i}\left(\frac{a}{2}+\lambda_{2j-1}+s_{2j-1}\right)\mathrm{e}^{-\mathrm{i}\theta_{2j-1}}\right),$$
$$\psi_{2j-1,2}=\mathrm{e}^{\frac{-\mathrm{i}\rho}{2}}\left(c\mathrm{e}^{-\mathrm{i}\theta_{2j-1}}+\mathrm{i}\left(\frac{a}{2}+\lambda_{2j-1}+s_{2j-1}\right)\mathrm{e}^{\mathrm{i}\theta_{2j-1}}\right),$$
$$\psi_{2j,1}=-\mathrm{e}^{\frac{\mathrm{i}\rho}{2}}\left(c\mathrm{e}^{\mathrm{i}\theta_{2j}}-\mathrm{i}\left(\frac{a}{2}+\lambda_{2j}+s_{2j}\right)\mathrm{e}^{-\mathrm{i}\theta_{2j}}\right),$$
$$\psi_{2j,2}=\mathrm{e}^{\frac{-\mathrm{i}\rho}{2}}\left(c\mathrm{e}^{-\mathrm{i}\theta_{2j}}-\mathrm{i}\left(\frac{a}{2}+\lambda_{2j}+s_{2j}\right)\mathrm{e}^{\mathrm{i}\theta_{2j}}\right), \tag{14}$$

where $\theta_j=s_j(x+d\lambda_j(y+4\lambda_j^2t)+b(a-2\lambda_j)t)$, $s_j=\sqrt{c^2+(a/2+\lambda_j)^2}$. To ensure that s_j is real, we set $c>\beta_j>0$ in this section. The breather solution and b-positon solution have been studied in Ref. [29]. In this section, two kinds of interaction are introduced, including the interaction between b-positon and breather, and the interaction between b-positons.

4.1. Interaction between b-positon and breather solutions

The hybrid solution of b-positon and breather can be derived through the limits $\lambda_{2j-1}\to\lambda_1=-a/2+\beta_1\mathrm{i}\,(j=1,\ldots,m,\ m\leqslant n-1)$ based on the n-breather solution which has been given in Ref. [29]. Now, let us have the following theorem.

Theorem 4 The order-n hybrid solution for the (2+1)-D cmKdV equations consisting of m-b-positon and l-breather can be written as

$$q^{[n]}_{mbp-lb}=c\mathrm{e}^{\mathrm{i}\rho}-2\mathrm{i}\frac{\Delta_{41}}{\Delta_{42}}, \tag{15}$$

with

$$\Delta_{41}=\left(\frac{\partial^{n_j}}{\partial\varepsilon^{n_j}}\Big|_{\varepsilon=0}(D_{2n})_{jk}(\lambda_j+\varepsilon)\right)_{2n\times 2n},$$
$$\Delta_{42}=\left(\frac{\partial^{n_j}}{\partial\varepsilon^{n_j}}\Big|_{\varepsilon=0}(W_{2n})_{jk}(\lambda_j+\varepsilon)\right)_{2n\times 2n},$$
$$\lambda_{2l-1}=\lambda_1\,(l\leqslant m),\quad n=m+l,$$
$$n_j=\begin{cases}\left[\dfrac{j-1}{2}\right], & j\leqslant 2m,\\ 0, & j>2m,\end{cases}$$

where $[\ \ ]$ means taking the integer part. D_{2n} and W_{2n} are given in Eq. (4), and ψ_{jk} are given in Eq. (14).

Substituting $n=3, m=2, \lambda_1=-a/2+\beta_1\mathrm{i}, \lambda_3=-a/2+\beta_2\mathrm{i}\,(\beta_j\in\mathbb{R})$ into Eq. (15), the order-3 hybrid solution consisting of positon and breather can be obtained. Figure 9 shows the evolution of $|q^{[3]}_{2bp-1b}|$ with time.

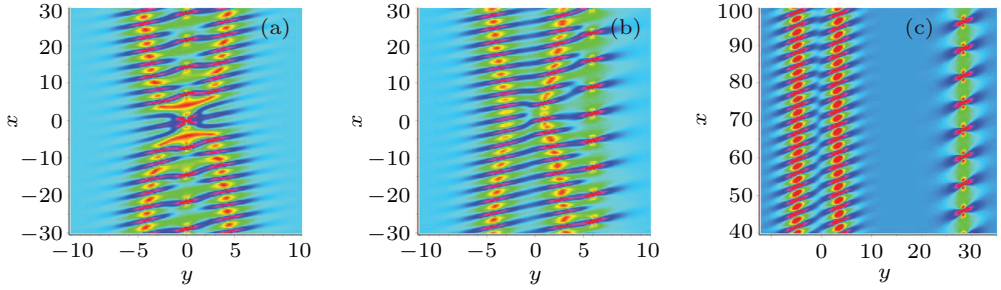


Fig. 9. The density figures of $|q^{[3]}_{2bp-1b}|$ with $a=b=c=d=1$, $\beta_1=1/2$, $\beta_2=9/10$: (a) $t=0$, (b) $t=2$, (c) $t=12$.

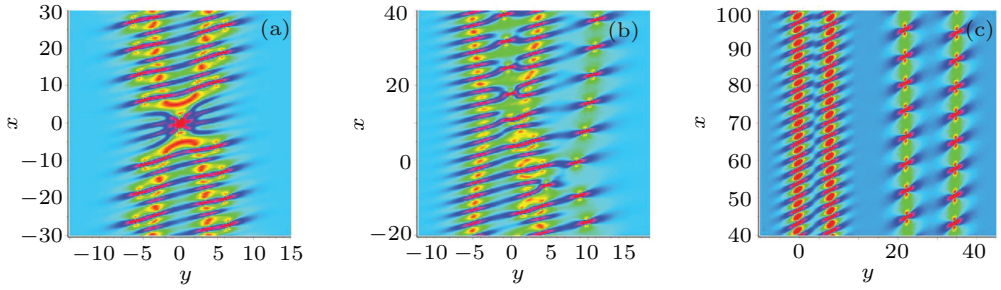


Fig. 10. The density figures of $|q^{[4]}_{2bp-2bp}|$ with $a=b=c=d=1$, $\beta_1=1/2$, $\beta_2=9/10$: (a) $t=0$, (b) $t=2$, (c) $t=12$.

4.2. Interaction between b-positon solutions

The hybrid b-positon solution are derived through the limits $\lambda_{2j-1}\to\lambda_1(j\leqslant m)$, $\lambda_{2j-1}\to\lambda_{2m+1}(j>m)$ using the order-n breather solution.

Theorem 5 The order-n hybrid b-positon solution for the (2+1)-D cmKdV equations consisting of m-b-positon and l-b-politon is obtained as

$$q^{[n]}_{mbp-lbp}=c\mathrm{e}^{\mathrm{i}\rho}-2\mathrm{i}\frac{\Delta_{51}}{\Delta_{52}}, \tag{16}$$

with

$$\Delta_{51}=\left(\frac{\partial^{n_j}}{\partial\varepsilon^{n_j}}\Big|_{\varepsilon=0}(D_{2n})_{jk}(\lambda_j+\varepsilon)\right)_{2n\times 2n},$$
$$\Delta_{52}=\left(\frac{\partial^{n_j}}{\partial\varepsilon^{n_j}}\Big|_{\varepsilon=0}(W_{2n})_{jk}(\lambda_j+\varepsilon)\right)_{2n\times 2n},$$
$$\lambda_{2l-1}=\begin{cases}\lambda_1, & l\leqslant m,\\ \lambda_{2m+1}, & l>m,\end{cases}$$
$$n=m+l,$$

$$n_j = \begin{cases} [\frac{j-1}{2}], & j \leqslant 2m, \\ [\frac{j-1}{2}] - m, & j > 2m, \end{cases}$$

where $[\quad]$ means taking the integer part and $\lambda_1 \neq \lambda_{2m+1}$. D_{2n} and W_{2n} are given in Eq. (4), and ψ_{jk} are given in Eq. (14).

Substituting $n=4$, $m=2$, $\lambda_1 = -a/2+\beta_1 \mathrm{i}$, $\lambda_3 = -a/2+\beta_2 \mathrm{i}$ ($\beta_j \in \mathbb{R}$) into Eq. (16), the order-4 hybrid b-positon solution containing two 2-b-positons can be obtained. Figure 10 shows the evolution of $|q^{[4]}_{2bp-2bp}|$ with time.

5. Conclusions

Taking the degenerate DT method into account, we have derived the positon solutions, hybrid solutions of positon and soliton, hybrid positon solutions, hybrid solutions of b-positon and breather, and hybrid b-positon solutions to the (2+1)-D cmKdV equation. The explicit form of n-positon solution is also given by Theorem 1. Then, the influences of different parameters are shown in Figs. 1 and 2. The composition of 2-positon and 3-positon solutions have been derived in Eqs. (9) and (11). Moreover, their numerical simulations are shown in Figs. 3–5. It is apparent that positon of (2+1)-dimensional NLLEs can be decomposed into multi-solitons just like (1+1)-dimensions. Further, the hybrid solution of positon and soliton is constructed in Theorem 2. The density figures of order-3 hybrid positon and soliton solutions with the same parameters except ξ_j are shown in Fig. 6. Also, the interaction between 2-positon and 1-soliton is discussed graphically in Fig. 7. After that, the order-n hybrid solution of m-positon and l-positon corresponding to different eigenvalues is constructed in Theorem 3. Several types of order-4 hybrid positon solutions with different parameters are proposed in Fig. 8. Lastly, the hybrid solutions on nonzero background, namely, the hybrid solution of b-positon, breather, and the hybrid b-positon solution are characterized by Theorems 4 and 5, respectively. The interaction between 2-b-positon and 1-breather is discussed graphically in Fig. 9. Moreover, the involution of order-4 hybrid b-positon solution with time is discussed graphically in Fig. 10. Bearing in mind the wide application of NLEEs, we hope the new results in this paper may provide a better understanding of physical applications associated with the (2+1)-D cmKdV equations.

Acknowledgements

Project sponsored by NUPTSF (Grant Nos. NY220161 and NY222169), the Foundation of Jiangsu Provincial Double-Innovation Doctor Program (Grant No. JSSCBS20210541), the Natural Science Foundation of the Higher Education Institutions of Jiangsu Province, China (Grant No. 22KJB110004), and the National Natural Science Foundation of China (Grant No. 11871446).

References

[1] Hobiny A and Abbas I A 2018 *Results Phys.* **10** 385
[2] Ma Y L, Wazwaz A M and Bang Q L 2021 *Math. Comput. Simul.* **187** 505
[3] Houwe A, Abbagari S, Doka S Y, Mustafa I and Bouetou T B 2021 *Chaos, Solitons Fractals* **151** 111254
[4] Rao J G, He J S and Cheng Y 2022 *Lett. Math. Phys.* **112** 75
[5] Rao J G, He J S and Malomed B A 2022 *J. Math. Phys.* **63** 013510
[6] Matveev V B 1992 *Phys. Lett. A* **166** 205
[7] Beutler R 1993 *J. Math. Phys.* **34** 3098
[8] Andreev V A and Brezhnev Y V 1995 *Phys. Lett. A* **207** 58
[9] Stahlhofen A A 1992 *Ann. Phys.* **504** 554
[10] Xing Q X, Wu Z W, Mihalache D and He J S 2017 *Nonlinear Dyn.* **89** 2299
[11] Yuan F 2020 *Nonlinear Dyn.* **102** 1761
[12] Matveev V B 2002 *Theor. Math. Phys. Fiz.* **131** 483
[13] Wang B, Zhang Z and Li B 2020 *Chin. Phys. Lett.* **37** 030501
[14] Matveev V B 1994 *J. Math. Phys.* **35** 2955
[15] Matveev V B 1992 *Phys. Lett. A* **166** 209
[16] Guo B, Ling L and Liu Q P 2012 *Phys. Rev. E* **85** 026607
[17] Wang X, Li Y and Chen Y 2014 *Wave Motion* **51** 1149
[18] Yang X Y, Zhang Z and Li B 2020 *Chin. Phys. B* **29** 100501
[19] Qiu Y Y, He J S and Li M H 2019 *Commun. Theor. Phys.* **71** 1
[20] Kumar S and Mohan B A 2021 *Phys. Scr.* **96** 125255
[21] Li B Q and Ma Y L 2020 *Appl. Math. Comput.* **386** 125469
[22] Rao J G, He J S, Mihalache D and Cheng Y 2019 *Appl. Math. Lett.* **94** 166
[23] Guo L J, He J S and Mihalache D 2021 *J. Phys. A: Math. Theor.* **54** 095703
[24] Guo L J, He J S, Wang L H, Cheng Y and Kevrekidis P G 2020 *Phys. Rev. Res.* **2** 033376
[25] Myrzakulov R, Mamyrbekova G, Nugmanova G and Lakshmanan M 2015 *Symmetry* **7** 1352
[26] Yesmakhanova K, Shaikhova G, Bekova G and Myrzakulov R 2017 *J. Phys. Conf. Ser.* **936** 012045
[27] Yuan F, Zhu X M and Wang Y L 2020 *Int. J. Appl. Math. Comput. Sci.* **30** 337
[28] Yuan F and Jiang Y 2020 *Mod. Phys. Lett. B* **34** 2050202
[29] Yuan F 2021 *Int. J. Mod. Phys. B* **35** 2150053
[30] Zhu X M 2020 *Commun. Nonlinear Sci. Numer. Simulat.* **91** 105438
[31] Yuan F 2021 *Mod. Phys. Lett. B* **35** 2150489
[32] Qiu D Q and Cheng W G 2019 *Commun. Nonlinear Sci. Numer. Simulat.* **78** 104887
[33] Song W J, Xu S W, Li M H and He J S 2019 *Nonlinear Dyn.* **97** 2135